



# Ultra-high pressure densification and properties of nanostructured SiC



Branko Matovic<sup>a,\*</sup>, Fatima Zivic<sup>b</sup>, Slobodan Mitrovic<sup>b</sup>, Dragan Prsic<sup>c</sup>, Vesna Maksimovic<sup>a</sup>, Tatjana Volkov-Husovic<sup>d</sup>, Ravi Kumar<sup>e</sup>, Nina Daneu<sup>f</sup>

<sup>a</sup> Institute of Nuclear Sciences Vinča, Department of Materials Sciences, Belgrade, Serbia

<sup>b</sup> Faculty of Engineering, University of Kragujevac, Serbia

<sup>c</sup> Faculty of Mechanical and Civil Engineering, University of Kragujevac, Kraljevo, Serbia

<sup>d</sup> Faculty of Technology and Metallurgy, University of Belgrade, Serbia

<sup>e</sup> Indian Institute of Technology-Madras (IIT Madras), Chennai, India

<sup>f</sup> Department for Nanostructured Materials Jožef Stefan Institute Jamova 39, 1000 Ljubljana Slovenia

## ARTICLE INFO

### Article history:

Received 12 June 2015

Received in revised form

4 September 2015

Accepted 9 September 2015

Available online 10 September 2015

### Keywords:

Structural

SiC ceramic

Sintering

Nanoparticles

X-ray techniques

## ABSTRACT

Cubic SiC nano-powder particles were synthesized by a sol–gel process with an average grains size of 9.5 nm which were subsequently densified by using a high-pressure “anvil-type with hollows” apparatus at a pressure of 4 GPa in order to obtain nanostructured bulk ceramic compacts. The density obtained was > 98% at a sintering temperature of 1500 °C with a holding time of only 60 s. The calculation of the average crystallite size ( $D$ ) was performed on the basis of the full width at half maximum intensity (FWHM) of the XRD peaks. Williamson–Hall plots were used to separate the effect of the size and strain in the nanostructured SiC compacts. Sintered nanostructured SiC ceramic exhibits hardness and elastic modulus of 32–420 GPa respectively. Wear properties were investigated and the average value of dynamic friction coefficient obtained was 0.16.

© 2015 Elsevier B.V. All rights reserved.

## 1. Introduction

Silicon carbide (SiC) possesses a good combination of thermo-mechanical and chemical properties due to its high covalency, which makes it one of the most useful materials for high temperature structural applications [1,2]. SiC is the fourth hardest material with low thermal expansion coefficient, good thermal conductivity and high fracture strength which can be retained even at temperatures above 1000 °C [3–5]. Its good thermal and chemical stability, excellent oxidation, corrosion and wear resistance and relatively good resistance to high neutron irradiation make SiC promising material for extremely harsh environments [6–10]. It is believed that these properties can be exploited at even higher temperatures, i.e., above 2000 °C if SiC can be protected by ultra-high temperature ceramics in the form of coatings (UHTCs) [11,12]. Also, ceramic materials with grain size in the nanoscale possess greater hardness and fracture strength, leading to immense interest in obtaining nanostructured bulk SiC ceramics [13,14].

As a consequence of the strong covalent bonding and extremely slow diffusivity, the properties of the SiC grains do not change up

to temperatures of 1700 °C [15,16]. However, the grain boundary phase already begins to soften at lower temperatures in a liquid phase sintered SiC. Depending on composition and amount of the grain boundary phase, various processes, such as diffusion, creep, slow crack growth, oxidation, corrosion, may occur at elevated temperatures with the consequence that a new defect population is generated, which determines the failure behavior and limits the lifetime. The extent to which these processes occur is mainly influenced by the refractoriness and viscosity of the amorphous grain boundary phase. Thus, one of the greatest drawbacks in the manufacturing of nanostructured SiC is the difficulty in sintering dense nanostructured ceramic without the use of sintering additives. The densification of nanocrystalline powders is a competition between the processes of densification and microstructure coarsening, which occur in parallel. To obtain SiC compacts free of any sintering additives and with full density, ultra-high pressure sintering techniques have been developed [17,18]. This process can reduce the sintering temperature and time activating solid state diffusion. Sintering at ultra-high pressures enables effective densification and sintering of the powder particles [19].

The objective of this paper is to fabricate nanostructured SiC ceramics free of any sintering additives by ultra-high pressure sintering method and investigate its mechanical properties.

\* Corresponding author.

E-mail address: [mato@vinca.rs](mailto:mato@vinca.rs) (B. Matovic).

## 2. Experimental

The starting material was high purity  $\beta$ -SiC powder fabricated by a sol–gel process [20]. In the present work, the source of silicon was TEOS (tetraethyl orthosilicate,  $\text{Si}(\text{OC}_2\text{H}_5)_4$ ) whereas the source of carbon was carbon cryogel. The carbon cryogel, was synthesized by polycondensation of resorcinol, R,  $\text{C}_6\text{H}_4(\text{OH})_2$  with formaldehyde, F, HCHO. RF solutions with TEOS were prepared by mixing in deionized water with carbon/silicon ratios: 1–1. RF sols with TEOS were decanted in glass tubes and aged at 85 °C for 4 days. The gels obtained after polymerization were carbonized at 800 °C in nitrogen flow and in order to obtain SiC, material was compacted and subjected to carbothermal reduction at 1200 °C for 1 h.

The mean grain size was 5 nm. The SiC nanopowder particles, after drying, were preliminarily consolidated into pellets of diameter 15 mm and height 5 mm under pressure of  $\sim 200$  MPa following high pressure (4 GPa) and annealing at 1500 °C using a Bridgman-type toroidal apparatus [21]. Apparatus is a simple design with two opposite flat surface where a pre-compacted powder specimen is mounted. It gives high pressure and, depending on the thickness of the specimen, high-pressure gradients due to the flow of the powder compact. The Bridgman anvil is set-up in vertical furnace, which can achieved high temperature with very fast heating and cooling rate (we used heating rate 300 °C/s and cooling rate was 20 °C/s).

The duration of the sintering process was 60 s. The sintered compacts were subsequently ground to remove remains of graphite after the technological process of sintering and to obtain the required quality and surface parallelism for physical and mechanical studies. The density of the sintered body was measured by the Archimedes method. The crystalline phases present in the raw powders, mixtures and sintered ceramics were identified by X-ray powder diffraction using a Rigaku diffractometer model UltimaIV (Ni-filtered Cu  $K_\alpha$  radiation;  $\lambda = 1.5406$  Å). The X-ray tube was operated at 40 kV and 40 mA. The diffractograms of the samples were recorded over the  $2\theta$  range from 20° up to 80° with the step of 0.02° and scanning time of 1 s per step.

Vickers macro-hardness was measured using LECO hardness tester by the indentation method with a load of 9.8 N and dwell time of 10 s. In order to determine the indentation toughness at least 15 Vickers indentation were introduced with load of 49 N. The indentation toughness was calculated from the lengths of radial cracks and indents diagonals using a formula valid for semi-circular crack system as proposed by Anstis [22].

Nano-hardness was determined by depth sensing quasistatic tests on a Hysitron Triboscope mounted on the scanner head of a atomic force microscope (AFM) using the Berkovich indenter. This device allows positioning of the indents with an accuracy of < 20 nm. Each sample was indented more than 50 times, and the imprints in the vicinity of microstructural defects (pores, removed grains, etc.) were excluded from the evaluation of measured data.

Dry linear reciprocating sliding contact between the flat sample of the SiC material and ruby ball was investigated. Normal loads of 500 and 1000 mN and linear speed of 12 mm/s were varied in dry conditions. Duration of each test was 10,000 cycles. Dynamic friction coefficient was recorded for each test and wear mechanisms were investigated.

## 3. Results and discussion

Fig. 1 shows that the XRD of the starting powder is SiC of type  $\beta$  (i.e., polytype 3C). Also, the additional diffraction peak was detected at  $2\theta = 33.6^\circ$ , which represents stacking faults on the {1 1 1} planes in cubic SiC crystals [23]. The calculation of the average

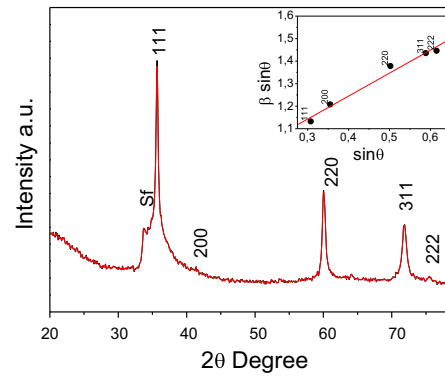


Fig. 1. XRD of as-prepared SiC powder, (SF-stacking fault) (the inset exemplifies the Williamson–Hall plot).

crystallite size ( $D$ ) was performed on the basis of the full width at half maximum intensity (FWHM) of the 111, 200, 220 and 311 reflections of cubic SiC by using Scherrer's formula:

$$D_{hkl} = \frac{K\lambda}{\beta \cos \theta} \quad (1)$$

where  $\lambda$  is the wavelengths of the X-rays used,  $\theta$  is diffraction angle,  $\beta$  is corrected half-width for instrumental broadening  $\beta = (\beta_m - \beta_s)$ ,  $\beta_m$  observed half-width and  $\beta_s$  is half-width of the standard  $\beta$ -SiC sample. The calculated crystallite size is about 9.5 nm.

Internal strain of starting SiC sample (as prepared at 1200 °C) and sintered sample at 1500 °C for 60 s was estimated from the Williamson–Hall plots, which were drawn using following equation [24]:

$$\beta_{total} \cos \theta = 0.9\lambda/D + 4\Delta d/d \sin \theta \quad (2)$$

where  $\beta_{total}$  is the full width half maximum of the XRD peak,  $\lambda$  is the incident X-ray wave length,  $\theta$  is the diffraction angle,  $D$  is the crystallite size and  $\Delta d$  is the difference of the  $d$  spacing corresponding to a typical peak. The obtained values of strain along with the values of crystallite size and lattice parameter are listed in Table 1. It is evident from Eq. (2) that the strain of nanocrystals,  $\Delta d/d$ , can be estimated from the slope of function  $\beta \cos \theta$  vs.  $\sin \theta$  whereas crystallite size,  $D$ , can be estimated from the y-intercept. As Table 1 shows, crystallite size as well as value for strain are significantly different for starting SiC powder and sintered SiC ceramic. This decrease in internal strain is considered to be the consequence of an ordering of atoms during sintering. Atomic ordering leads to a reduction in the concentration of dislocations. Furthermore, it is well known that the significant amount of strain is localized at the surface of crystallites as a result of a high concentration of broken bonds. Therefore, it is expected that the internal strain decreases with an increase in crystallite size due to decrease in the surface area of crystallites.

The XRD of sample sintered at 1500 °C for 1 min under the pressure of 4 GPa (Fig. 2) depict sharpened diffraction lines resulting from increased the crystalline size. The calculated crystalline size is about 42 nm.

Low-magnification TEM image of the sample sintered at

Table 1  
Crystallite size and lattice strain of as-synthesized powder and sintered SiC ceramic at 1500 °C for 1 min.

| Temperature (°C)              | As-synthesized       | 1500                 |
|-------------------------------|----------------------|----------------------|
| Crystallite size (nm)         | 9.5                  | 42                   |
| Lattice strain ( $\epsilon$ ) | $6.02 \cdot 10^{-3}$ | $5.29 \cdot 10^{-3}$ |

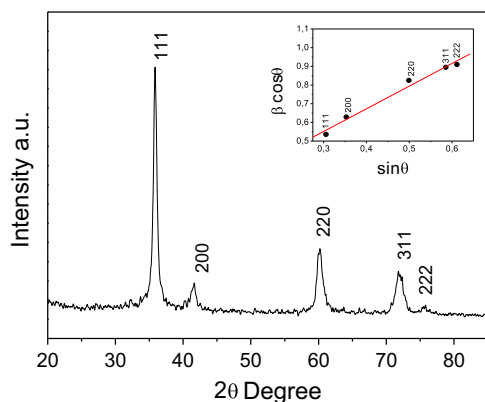


Fig. 2. XRD of sintered SiC ceramic at 1500 °C for 1 min (the inset exemplifies the Williamson-Hall plot).

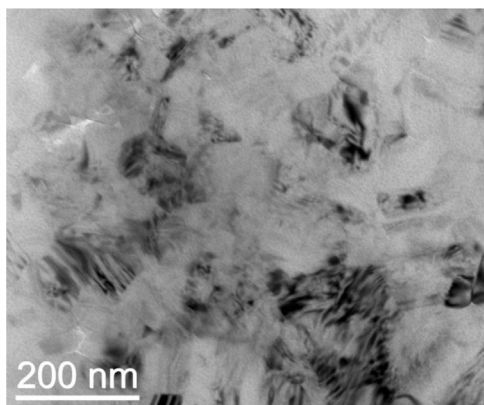


Fig. 3. Transmission electron micrograph of SiC sintered at 1500 °C for 1 min.

1500 °C is shown in Fig. 3. It reveals that very large pore-free areas were observed in the sample, indicating effective densification process under the ultra-high pressure. The main SiC phase is the cubic modification 3C-SiC or  $\beta$ -SiC, as already shown by XRD analyses. However,  $\beta$ -SiC grains contain many hexagonal-type defects. The majority of the SiC grains are about 50 nm and they are in a direct contact without the presence of any amorphous or secondary phase at the grain boundaries, which is a very important for the mechanical and properties of the obtained ceramic.

The effect of pressure has a direct influence on particle redistribution, the elimination of pores and the destruction of agglomerates [25] for SPS, therefore, it is expected that the applied pressure has a more pronounced influence on the densification compared to SPS. Therefore, it is not surprising that the sample sintered at 1500 °C for only 60 s exhibits such high relative density (> 98%).

The micro-hardness and the fracture toughness for this sample are 25.38 GPa and 4.42 MPa m<sup>1/2</sup>, respectively. Also a very high of elastic modulus (420 GPa) is obtained. The obtained value for micro-hardness is very high and moderate value for fracture toughness. Nano-SiC ceramics obtained under high pressure (2–8 GPa) at temperature at 1200 °C for 60 s [26] showed that the microhardness of ceramics increases depending of applied pressure (2–8 GPa) from 7.6 to 17 GPa, respectively. In the other side, densification process at 1200 °C is not effective enough to create strong chemical bonding at the nano-particles interfaces during sintering time of 60 s.

However, nano-hardness is significantly higher in comparison with macro-hardness measurement (32 GPa). This disagreement can be explained by influence of several factors such as microstructure, hardness of individual grains, indentation size effect,

grain boundaries, that cause a larger scatter in case of micro-hardness testing. As reported in literature, value for nano-hardness obtained in this study (ultra high pressure at 1500 °C) is comparable with nano-hardness (33 GPa) obtained by liquid phase sintered SiC. However this ceramic is sintered by using Y<sub>2</sub>O<sub>3</sub> and Yb<sub>2</sub>O<sub>3</sub> additive system (15 wt%) and hot pressed at 1850 °C for 1 h under mechanical pressure of 30 MPa in Ar+N<sub>2</sub> atmosphere and annealed for 10 h at 1850 °C in Ar+N<sub>2</sub> atmosphere [27].

The average values of dynamic friction coefficient were 0.16 for the sintered ceramic sample. Long running-in periods was exhibited for sample with stable friction coefficient curve. Very mild adhesive wear was observed as the governing wear mechanism, together with a very low abrasive wear in a form of a few shallow scratches along the wear tracks. In general, a very low wear behavior was exhibited for all tests.

#### 4. Conclusions

High pressure sintering of  $\beta$ -silicon carbide nanoparticles has been reported in this work. Densification of green compact has been achieved without addition of sintering aids. A relative density of about 98% of has been obtained by applying a high pressure of 4 GPa at 1500 °C for 1 min. The microstructure of the obtained sintered SiC shows no porosity with grain size in nano range. Sintered material is a monolithic nanocrystalline SiC ceramic. High values for nano-hardness (32 GPa) as well as elastic modulus (420 GPa) has been obtained. Tribological tests showed that monolithic nanocrystalline SiC ceramic has a potential for application in extreme conditions.

#### Acknowledgment

This project was financially supported by the Ministry of Education and Science of Serbia (Project number: 45012). This work has been enabled through the Slovenian-Serbian bilateral collaboration under the project No. BI-RS/12-13-019: 'Minerals as precursors for advanced technologies'.

#### References

- [1] W.D.G. Böcker, Covalent high-performance ceramics, *Adv. Mater.* 4 (1992) 169–178.
- [2] K.A. Schwetz, Silicon carbide based hard materials, in: R. Riedel (Ed.), *Handbook of Ceramics Hard Materials*, Wiley-VCH, 2000.
- [3] Y. Hirata, Theoretical analyses of thermal shock and thermal expansion coefficients of metals and ceramics, *Ceram. Int.* 41 (2015) 1145–1153.
- [4] Y. Li, J. Yin, H. Wu, P. Lu, Y. Yan, X. Liu, Z. Huang, D. Jiang, High thermal conductivity in pressureless densified SiC ceramics with ultra-low contents of additives derived from novel boron-carbon sources, *J. Eur. Ceram. Soc.* 34 (2014) 2591–2595.
- [5] Y. Umeno, A. Kubo, S. Nagao, Density functional theory calculation of ideal strength of SiC and GaN: effect of multi-axial stress, *Comput. Mater. Sci.* 109 (2015) 105–110.
- [6] D. Woodilla, M. Buonomo, I. Bar-On, Elevated temperature behaviour of high-strength silicon carbide, *J. Am. Ceram. Soc.* 76 (1993) 249–252.
- [7] H. Tanaka, Silicon carbide powder and sintered materials, *J. Ceram. Soc. Jpn.* 119 (2011) 218–233.
- [8] B. Matovic, T. Yano, Chapter 3.1 – silicon carbide and other carbides, 2nd ed., in: S. Somiya (Ed.), *From Stars to the Advanced Ceramics Handbook of Advanced Ceramics*, Oxford, 2013, pp. 225–244.
- [9] H. Tanaka, T. Iseki, *Advanced Silicon Carbide Ceramics*, Japan Soc Promo Science, The 124th Committee, Uchida Roukaku Publ., Tokyo, 2001, pp. 339–346.
- [10] T. Yano, B. Matovic, Chapter X: advanced ceramics for nuclear applications, 2nd ed., in: S. Somiya (Ed.), *From Stars to the Advanced Ceramics Handbook of Advanced Ceramics*, Oxford, 2013, pp. 1–38.
- [11] E. Wuchina, E. Opila, M. Opeka, W. Fahrenholtz, I. Talmy, UHTCs ultra-high temperature ceramic materials for extreme environment applications, *Electrochem. Soc. Interface* 16 (2007) 30–36.
- [12] K. Upadhyay, J.M. Yang, W. Hoffman, *Materials for ultrahigh temperature*

- structural applications, *Am. Ceram. Soc. Bull.* 76 (1997) 51–56.
- [13] R. Vassen, D. Stover, Processing and properties of nanograin silicon carbide, *J. Am. Ceram. Soc.* 82 (1999) 2585–2593.
- [14] Y. Shinoda, T. Nagano, F. Wakai, Fabrication of nanograin silicon carbide by ultra-pressure hot isostatic pressing, *J. Am. Ceram. Soc.* 82 (1999) 771–773.
- [15] Y.W.H. Lee, X.H. Yao, First principle investigation of phase transition and thermodynamic properties of SiC, *Comput. Mater. Sci.* 106 (2015) 76–82.
- [16] O. Ravkina, J. Räthel, A. Feldhoff, Influence of different sintering techniques on microstructure and phase composition of oxygen-transporting ceramic, *J. Eur. Ceram. Soc.* 35 (2015) 2833–2843.
- [17] S. Grasso, T. Saunders, H. Porwal, M. Reece, Ultra-high temperature spark plasma sintering of  $\alpha$ -SiC, *Ceram. Int.* 41 (2015) 225–230.
- [18] L.G. Khvostantsev, V.A. Sidorov, O.B. Tsiok, High pressure toroid cell. Applications in planetary and material sciences, in: M.H. Manghnani, T. Yagi (Eds.), *Properties of earth and planetary materials at high pressure and temperature*, Geophys. Monogr. Ser. 101, vol. 101, AGU, Washington, DC, 1998.
- [19] G. Lian, L. Wei, W. Hongzi, Preparation of Y-ZrO<sub>2</sub> nano-grain by super-high pressure compaction, *J. Inorg. Mater.* 15 (2000) 1005–1008.
- [20] B. Babić, D. Bučevac, A. Radosavljević-Mihajlović, A. Došen, J. Zagorac, J. Pantić, B. Matović, New manufacturing process for nanometric SiC, *J. Eur. Ceram. Soc.* 32 (2012) 1901–1906.
- [21] E.K. Graham, Recent developments in conventional high-pressure methods, *J. Geophys. Res.* 91 (1986) 4630–4642.
- [22] G.R. Anstis, P. Chantikul, B.R. Lawn, D.B. Marshall, A evolution of indentation techniques for measuring fracture toughness. I. Direct crack measurement, *J. Am. Ceram. Soc.* 64 (1981) 533–538.
- [23] Q. Lu, J. Hu, K. Tang, Y. Oian, G. Zhou, X. Liu, J. Zhu, Growth of SiC nanorods at low temperature, *Appl. Phys. Lett.* 75 (1999) 507–512.
- [24] C. Suryanarayana, M. Grant Norton, *X-ray Diffraction: A Practical Approach*, Springer, New York, 1998.
- [25] Z.A. Munir, The effect of electric field and pressure and consolidation of materials: a review of the spark plasma sintering method, *J. Mater. Sci.* 41 (2006) 763–777.
- [26] A. Swiderska-Sroda, G. Kalisz, B. Palosz, N. Herlin-Boime, SiC nano-ceramics sintered under high-pressure, *Rev. Adv. Mater. Sci.* 18 (2008) 422–424.
- [27] M. Balog, P. Sajgalik, M. Hnatko, Z. Lences, F. Monteverde, J. Keckes, J.L. Huang, Nano- vs. micro-hardness of liquid phase sintered SiC, *J. Eur. Ceram. Soc.* 25 (2005) 529–534.